Phase Behavior of Linear/Branched Polymer Blends

N. Clarke*

Department of Physics, University of Sheffield, Sheffield S3 7RH, U.K.

T. C. B. McLeish

Department of Physics and Polymer IRC, University of Leeds, Leeds LS2 9JT, U.K.

S. D. Jenkins

ICI Wilton Research Centre, Wilton, Middlesbrough, Cleveland TS6 8JE, U.K.

Received August 17, 1994; Revised Manuscript Received February 22, 1995®

ABSTRACT: The phase behavior of a linear/branched polymer blend is predicted within the framework of the Flory–Huggins theory. The linear polymer is treated as monodisperse and the branched polymer as polydisperse with power law statistics, $\phi(N) \propto N^{-(\tau-1)}$, cut off at some upper degree of polymerization N_2. The latter is dependent on the reacted fraction, α, and the functionality, f, of the functional groups of the branched polymer. We calculate analytically the spinodal curves for various α up to the gel point and find unusual behavior of the critical point. In particular, it is found to be very sensitive to the exponent of the power law distribution function, e.g., whether τ takes the classical value of 2.5 or the percolation value of 2.20. Example cloud point curves and coexistence curves have been calculated numerically, again for various α, and a picture of the evolution of the phase diagram during cross-linking has been constructed. The coexistence curves are surprisingly steep as χ is varied over a large range; this is particularly evident for the parameters of the linear-rich phase. Hence it is found that although the distribution of the branched polymer in the linear-rich phase varies considerably with increasing χ, the ratio of linear and branched polymer volume fractions within this phase does not. From our results we are able to predict, at least qualitatively, a "secondary" phase separation that is known to occur in such blends.

1. Introduction

The toughness of a cross-linked epoxy resin may be dramatically increased by the incorporation of a thermoplastic at the precuring stage of processing. The phase behavior of such a blend can be utilized to produce interesting and mechanically useful morphologies; hence an understanding of the phase diagram and its evolution during the curing process is very important.

The phase behavior of a typical polymer blend is well described, at least qualitatively, by the theory of Flory[1] and Huggins,[2] in which the free energy of mixing for a polymer blend is written as

$$\frac{F_{\text{mix}}}{k_B T} = \frac{\phi_A}{N_A} \ln \phi_A + \frac{\phi_B}{N_B} \ln \phi_B + \chi \phi_A (1 - \phi_A) \quad (1.1)$$

where ϕ_A and ϕ_B are the volume fractions and N_A and N_B are the degrees of polymerization of polymers A and B, respectively. χ is some interaction parameter which for many blends is related to temperature by

$$\chi = a + \frac{b}{T} \quad (1.2)$$

where a is an entropic term and b is an enthalpic term. For the sake of simplicity, we assume χ to be independent of concentration.

The phase diagram is determined by finding the state which minimizes the free energy for any given composition and value of χ. It is characterized by two curves: the "binodal" and the "spinodal" (see Figure 1). Below the binodal curve the mixed phase is stable and the blend is considered to be miscible. Between the binodal and the spinodal curves the mixed phase is metastable, i.e., the total free energy of the blend may be lowered by phase separation, but a potential barrier must be overcome first. Within the region of the spinodal curve the mixed state is completely unstable. Where the two curves meet, the critical point, the tie line connecting coexisting phases becomes a point.

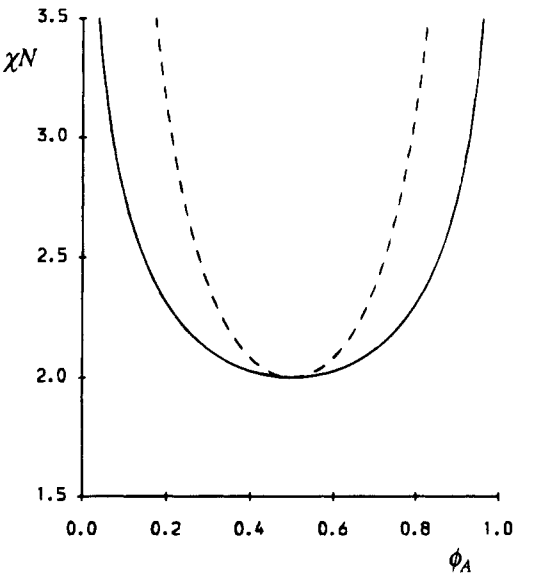

Figure 1. Phase diagram of a symmetric ($N_A = N_B = N$) monodisperse polymer blend. Within the spinodal curve (- - -) the mixed state is unstable, and between the spinodal curve and the binodal curve (—) the mixed state is metastable.

For a relation such as eq 1.2 a blend phase separates on quenching and the critical point is the upper temperature at which phase separation occurs (upper critical solution temperature (UCST) behavior). How-

* Present address: Faculty of Mathematical Studies, University of Southhampton, Southhampton SO17 1BJ, U.K.

® Abstract published in *Advance ACS Abstracts,* May 1, 1995.

0024-9297/95/2228-4650$09.00/0

ever, it is well known that many blends phase separate on heating, so that the critical point is the lowest temperature of phase separation (lower critical solution temperature (LCST) behavior). The latter can be explained, phenomenologically, within the framework of the simple theory described above if $b < 0$. Many other attempts to predict LCST behavior exist, both as extensions to Flory–Huggins theory or using equation of state theories (for a review, see ref 3).

In a thermoset/thermoplastic blend the components are usually mixed together and the cross-linking of the epoxy occurs *in situ*. Assuming the blend to be initially miscible, the increase of the molecular weight of the epoxy during curing may result in phase separation, even if the temperature is kept constant, due to the decrease of the entropy of mixing of the epoxy component. Eventually the epoxy forms an infinite network (at the gel point) and any further phase separation is suppressed: a "quasi-equilibrium" structure becomes "frozen" in.

The resultant morphology is strongly dependent on the dynamics of phase separation; in particular, a quench from the miscible one-phase region into the metastable region or into the unstable region results in nucleation and growth or spinodal decomposition, respectively. For a blend which crosses and remains within the metastable region, the structure will be either an epoxy network dispersed with thermoplastic droplets (reinforced rubber) or a continuous thermoplastic matrix dispersed with epoxy droplets (impact-resistant plastics). However, if the blend crosses into the unstable region of its phase diagram, the structure will be cocontinuous with unique mechnical properties.

Many experimental studies have looked at these systems,[4-7] but, due to the complex interaction between phase separation and cross-linking, there have been few theoretical attempts to explain the behavior. Binder and Frisch[8] considered the phase behavior of a blend in which the thermoset had formed a complete "weakly" cross-linked network before phase separation could take place. This required the introduction of an elastic term into the free energy. A similar method was used by Donatelli et al.[9] to semiempirically derive phase domain sizes. Teng and Chang[7] and Williams et al.[10] have proposed models for phase separation prior to network formation in which only the average molecular weight of the thermoset during curing is considered. In a previous paper[11] we calculated the growth rate of concentration fluctuations in star/star and star/linear polymer blends and concluded that the dynamics of entangled branched polymers are very important in the early stages of spinodal decomposition. Recently, Tanaka and Stockmayer[12] have considered thermoreversible gels in blends, and the interaction between the gel point and phase separation. The distribution of cluster sizes is a functional of the minimum free energy state, unlike chemically cured branched polymers, which we consider in this paper, in which cluster size distribution is dependent only on cure time. Such a difference will produce major qualitative differences in the phase behavior.

In this paper we calculate phase diagrams of a thermoset/thermoplastic blend prior to the gel point using Flory–Huggins theory, treating the thermoset as a polydisperse branched polymer with power law statistics (see section 2). The thermoplastic component is assumed to be a monodisperse linear polymer. A more exact approach would consider the system as a complex ternary blend:thermoplastic/epoxy/curing agent; however, for simplicity, we assume it to be a binary blend in which the epoxy and curing agent form a polydisperse component. We hope to extend the study we present in this paper to look at postgel effects, by incorporating q-dependent elastic terms into the free energy and considering microphase separation. Within the scope of this work, elastic effects can only enter into the kinetics of segregation.

The Flory–Huggins theory was extended by Koningsveld and Staverman[13] and later by Solc[14,15] to allow for the effects of polydispersity in linear polymer blends. We further extend this method to account for polydispersity in linear/branched blends in section 3. We calculate the spinodal curve and the critical point analytically, and then in section 4 we present the numerical method and results for the calculation of the coexistence conditions and the distribution of the branched polymer into the two phases. Finally, we discuss how our results may explain, at least qualitatively, the phenomena of secondary phase separation observed in some blends.

2. Branched Polymer Statistics

Within a cross-linked polymer system there is a very large spread in the size of the macromolecules present. The volume fraction occupied by branched polymers of a given degree of polymerization has been calculated by Flory[16] and Stockmayer.[17] In their theory bonds between monomers are formed, with some probability, on a treelike structure (a Bethe lattice). A consequence of such a model is that cyclic bonds do not occur and excluded volume effects are ignored. The resultant distribution function of this "classical" theory is

$$\phi(N) = [(fN - N)!f/(N - 1)!(fN - 2N + 2)!]\alpha^{N-1} \times (1 - \alpha)^{fN-2N+2} \quad (2.1)$$

where f is the functionality and α is the reacted fraction of the functional groups (or the conversion factor). This can be approximated as

$$\phi(N) = k'A^N N^{-3/2} \quad (2.2)$$

where k' is a normalization constant, and

$$A \equiv (1 - \alpha)^{f-2}\alpha(f - 1)^{f-1}/(f - 2)^{f-2} \quad (2.3)$$

Since $A < 1$ the term A^N of eq 2.2 acts as an upper cutoff to the power law at some value N_2 which is related to the conversion factor and the functionality by

$$N_2 \sim -[\ln A]^{-1} \quad (2.4)$$

The degree of polymerization of the un-cross-linked thermoset is represented by a lower cutoff N_1. Hence the distribution function is

$$\phi(N) = kN^{-\tau+1}; \quad N_1 \le N \le N_2$$

$$\phi(N) = 0; \quad N < N_1, N > N_2 \quad (2.5)$$

where the exponent, τ, familiar in the context of critical phenomena, has been introduced. It is commonly used to denote the scaling behavior of the number of branched polymers of a given size, i.e., $n(N) \sim N^{-\tau}$, and hence $\phi(N) \sim N^{-\tau+1}$.

Recently, attention has focused on a new class of models which come under the heading of "percolation theory".[18] This model allows for the effects of cyclic bonds and excluded volume by considering bond percolation on a regular lattice and determining the resultant scaling behavior near the gel point using numerical methods and simulations.

In the classical theory of Flory and Stockmayer, $\tau = 2.5$; however, percolation theory predicts $\tau \approx 2.20$. The applicability of the two theories has been discussed by de Gennes,[19] who looked at the limits of the mean field theory by using the Ginzburg criteria. It was predicted that as the gel point is approached, there will always be a crossover from classical to percolation statistics. However, for the process of vulcanization, which is the cross-linking of long linear polymers, classical statistics are valid. The reason for this is that within polymer melts, as has already been noted, the effects of excluded volume are screened out. While it is not clear that a strong meaning can be attached to nonclassical statistics within the Flory–Huggins mean field theory, it is interesting, as a "first-order" study, to consider the effects of $\tau \neq 2.5$, on various analytical results. However, when calculating phase diagrams, we shall focus our attention on the classical Flory–Stockmayer statistics. Near the gel point itself, even these statistics break down because gelation clusters have a fractal dimension of 4. Mean field results are constrained to a range of molecular weights bounded by a maximum, given by the Ginzburg argument due to de Gennes.[19] Even nonclassical distributions of branched polymers will have a range of molecular weights (or, equivalently, range of branching density away from the percolation transition) in which local composition fluctuations are screened and in which a Flory–Huggins free energy is valid.

The normalization constant k of eq 2.5 is found from the condition

$$\int_{N_1}^{N_2} \phi(N) = 1 - \phi_{\text{lin}} \tag{2.6}$$

therefore,

$$k = \frac{(\tau - 2)(1 - \phi_{\text{lin}})}{N_1^{-(\tau-2)} - N_2^{-(\tau-2)}} \tag{2.7}$$

One of the features of branched polymers of particular interest is the onset of gelation, described theoretically by the appearance of a molecule of "infinite" size which spans the entire polymer network. It is well known that this occurs at a critical value of α given by

$$\alpha_c = 1/(f - 1) \tag{2.8}$$

From eqs 2.3, 2.4, and 2.8 it can be seen that at the gel point

$$A \equiv 1 \quad \text{and} \quad N_2 \to \infty \tag{2.9}$$

Hence in this limit eq 2.5 becomes exact, and although it may be considered a crude approximation away from the gel point, it has the advantage that the two parameters a and f have been replaced by just one, $N_2 = N_2(a,f)$.

The distribution of any polydisperse polymer is usually characterized by three averages,

$$\bar{N}_n = \frac{\sum_i \phi_i}{\sum_i \phi_i/N_i}; \quad \bar{N}_w = \frac{\sum_i \phi_i N_i}{\sum_i \phi_i}; \quad \bar{N}_z = \frac{\sum_i \phi_i (N_i)^2}{\sum_i \phi_i N_i} \tag{2.10}$$

which are referred to as the number (n), w, and z averages, respectively. The summations are over all the components of the branched polymer. For a continuous distribution function, such as that of eq 2.5, the summations may be replaced by integrals with appropriate limits. We shall also seen in the next section that all our calculations may be performed in terms of the ratios $n_1 = N_1/N_{\text{lin}}$ and $n_2 = N_2/N_{\text{lin}}$, where N_{lin} is the degree of polymerization of the linear polymer (the thermoplastic). Consequently, the averages may be written as

$$\bar{n}_n \equiv \frac{\bar{N}_n}{N_{\text{lin}}} = \frac{\tau - 1}{\tau - 2}\left[\frac{n_1^{2-\tau} - n_2^{2-\tau}}{n_1^{1-\tau} - n_2^{1-\tau}}\right] \tag{2.11}$$

$$\bar{n}_w \equiv \frac{\bar{N}_w}{N_{\text{lin}}} = \frac{\tau - 2}{\tau - 3}\left[\frac{n_1^{3-\tau} - n_2^{3-\tau}}{n_1^{2-\tau} - n_2^{2-\tau}}\right] \tag{2.12}$$

$$\bar{n}_z \equiv \frac{\bar{N}_z}{N_{\text{lin}}} = \frac{\tau - 3}{\tau - 4}\left[\frac{n_1^{4-\tau} - n_2^{4-\tau}}{n_1^{3-\tau} - n_2^{3-\tau}}\right] \tag{2.13}$$

At the gel point the number average scales as n_1, independently of τ, but the w and z averages diverge. This has important consequences for the behavior of the spinodal curve and critical point, as will be shown in the next section.

3. Thermodynamics

If one of the components of a polymer blend is polydisperse, the corresponding expression to eq 1.1, the free energy of mixing, may be written as[13,14]

$$\frac{F_{\text{mix}}}{k_B T} = \frac{\phi_{\text{lin}}}{N_{\text{lin}}} \ln \phi_{\text{lin}} + \sum_i \frac{\phi_i}{N_i} \ln \phi_i + \chi \phi_{\text{lin}}(1 - \phi_{\text{lin}}) \tag{3.1}$$

where ϕ_{lin} is the volume fraction of linear polymer of degree of polymerization N_{lin}, ϕ_i is the volume fraction of the ith component of the branched polymer of degree of polymerization N_i, and the sum is over all the different sizes of branched polymer. From this expression it is possible to determine all the features of the phase diagram, i.e., the spinodal curve, the critical point, and the coexistence conditions.

3.1. The Spinodal Curve and the Critical Point. As was discussed in the Introduction, the spinodal curve represents the boundary within which the mixed state is completely unstable. For a simple binary blend the spinodal is the locus of points on the phase diagram for which the curvature of the free energy is zero. It was shown by Gibbs[20] that the corresponding requirement for a multicomponent blend is

$$Y = \left|\frac{\partial^2 F}{\partial \phi_i \partial \phi_j}\right| = 0 \tag{3.2}$$

i.e., the determinant of the matrix formed by the second

derivative of the free energy with respect to each component is equal to zero. It follows from eq 3.1 that the spinodal curve is given by[13]

$$\chi_s N_{lin} = \frac{1}{2}\left[\frac{1}{\phi_{lin}} + \frac{1}{(1-\phi_{lin})\bar{n}_w}\right] \tag{3.3}$$

and only depends on the w average. This expression is very similar to that for a binary monodisperse blend with the degree of polymerization of one of the components simply replaced by the average $\bar{N}_w$ of the polydisperse component.

At the critical point the spinodal and binodal curves meet. For a binary monodisperse blend this is the minimum of the two curves (see Figure 1); in other words, the derivative of the curvature of the free energy with respect to composition is zero. The extension of this requirement for a polydisperse blend is[20]

$$Y' = 0 \tag{3.4}$$

where Y' is formed from the determinant of eq 3.2 by replacing any one of the rows by the derivative of Y with respect to the appropriate volume fraction. Hence[13]

$$\phi_{lin}^{crit} = \left[1 + \frac{\bar{n}_z^{1/2}}{\bar{n}_w}\right]^{-1} \tag{3.5}$$

and

$$\chi^{crit} N_{lin} = \frac{1}{2}\left[\frac{1}{\phi_{lin}^{crit}} + \frac{1}{(1-\phi_{lin}^{crit})\bar{n}_w}\right] \tag{3.6}$$

It is interesting to consider how the spinodal curve and the critical point behave as the gel point is approached. Using our expression for the w average, eq 2.12 in the limit of large N_2, we can see that near the gel point the spinodal curve is given by

$$\chi_s N_{lin} \to \frac{1}{2\phi_{lin}} \qquad \{\phi_{lin} \neq 1\} \tag{3.7}$$

The behavior of the critical point is crucially dependent on the value of τ, in particular whether it is less than, equal to, or greater than the classical value of 2.5. From eqs 3.5 and 3.6 we find

(i) $\tau < 2.5$ (percolation statistics)

$$\phi_{lin}^{crit} \to 1; \quad N_{lin}\chi^{crit} \to \frac{1}{2} \tag{3.8}$$

(ii) $\tau = 2.5$ (classical statistics)

$$\phi_{lin}^{crit} \to \left[1 + \frac{1}{\sqrt{3}} n_1^{-1/2}\right]^{-1}; \quad N_{lin}\chi^{crit} \to \frac{1}{2}\left[1 + \frac{1}{\sqrt{3}} n_1^{-1/2}\right] \tag{3.9}$$

(iii) $\tau > 2.5$

$$\phi_{lin}^{crit} \to 0; \quad N_{lin}\chi^{crit} \to \infty \tag{3.10}$$

In cases i and ii the critical point tends toward a well-defined value, and in cases i and iii it is independent of composition, whereas for $\tau = 2.5$ it is a function of n_1. The trajectories of the critical point during polymerization are illustrated for all three possibilities in Figure 2. As far as we are aware, only the first two correspond to physical theories.

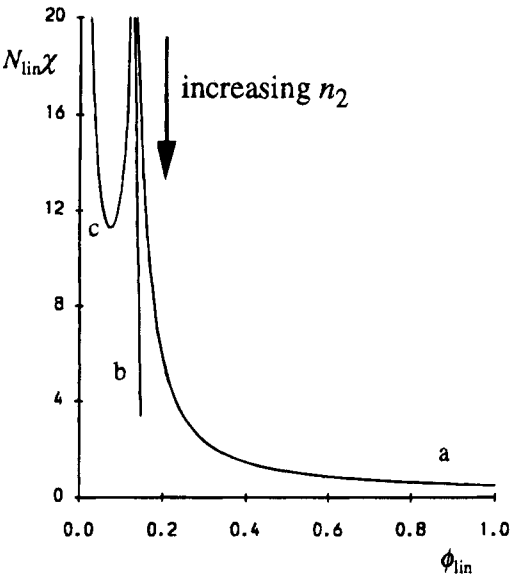

Figure 2. Behavior of the critical point (see section 3.1) of a linear/branched polymer blend as n_2 increases with $n_1 = 0.01$: (a) $\tau < 2.5$; (b) $\tau = 2.5$; (c) $\tau > 2.5$.

It is clear from Figure 2 that, for $\tau = 2.5$, ϕ_{lin}^{crit} does not increase very much as $n_2 \to \infty$; in fact, from eq 3.5 it can be seen that in the opposite extreme, which represents the blend prior to any cross-linking, i.e., when $n_2 = n_1$,

$$\phi_{lin}^{crit} = [1 + n_1^{-1/2}]^{-1} \tag{3.11}$$

It is also worth noting that for $\tau < 2.5$ the critical point becomes the minimum of the spinodal curve at the gel point. The only other system, of which we are aware, exhibiting this behavior is a binary monodisperse polymer blend.

3.2. Coexistence Conditions. The composition of demixed phases may be determined from the condition that for two phases of different compositions to coexist, at a fixed χ, the thermodynamic chemical potential of each component in each phase must be equal, i.e.,

$$\mu_{lin}(\text{linear-rich}) = \mu_{lin}(\text{branch-rich})$$

$$\mu_i(\text{linear-rich}) = \mu_i(\text{branch-rich}) \quad \text{for all } i \tag{3.12}$$

where for any polymer component k

$$\mu_k \equiv \left.\frac{\partial F_{mix}}{\partial n_k}\right|_{n_{j\neq k}} = F_{mix} - \sum_{j\neq k}\phi_j \frac{\partial F_{mix}}{\partial \phi_j} + (1-\phi_k)\frac{\partial F_{mix}}{\partial \phi_k} \tag{3.13}$$

Equating the chemical potentials of the linear polymer in each phase using eq 3.1 and eqs 3.12 and 3.13 gives

$$\ln \phi_{lin}' + (1-\phi_{lin}')\left[1 - \frac{1}{\bar{n}_n'}\right] + N_{lin}\chi(1-\phi_{lin}')^2 = \ln \phi_{lin}'' + (1-\phi_{lin}'')\left[1 - \frac{1}{\bar{n}_n''}\right] + \chi N_{lin}(1-\phi_{lin}'')^2 \tag{3.14}$$

and similarly for each component of the branched

polymer, i,

$$\frac{N_{lin}}{N_i}\ln\phi_i' - \phi_{lin}' - \frac{1-\phi_{lin}'}{\bar{n}_n'} + N_{lin}\chi\phi_{lin}'^2 = \frac{N_{lin}}{N_i}\ln\phi_i'' - \phi_{lin}'' - \frac{1-\phi_{lin}''}{\bar{n}_n''} + N_{lin}\chi\phi_{lin}''^2 \quad (3.15)$$

The parameters of the branch-rich and linear-rich phases are denoted by a single prime and a double prime, respectively. The number-average degrees of polymerization of the branched polymer in each phase, $\bar{n}_n'$ and $\bar{n}_n''$, is found by applying the definition of eq 2.10 to the distribution within each phase.

Requiring that the total amount of both components is distributed between the two phases leads to the condition of "material balance"[16]

$$\frac{V''}{V}\phi_i'' = \frac{\phi_i}{1 + r(\phi_i'/\phi_i'')} \quad (3.16)$$

where $r = V'/V''$ and,

$$\frac{\phi_i'}{\phi_i''} = \exp\left\{\sigma\frac{N_i}{N_{lin}}\right\} \quad (3.17)$$

In eq 3.17 σ is the "separation factor" given by

$$\sigma = 2N_{lin}\chi(\phi_{lin}'' - \phi_{lin}') + \ln(\phi_{lin}'/\phi_{lin}'') \quad (3.18)$$

After substitution of $n = N/N_{lin}$ into eq 3.17 and integration of eq 3.16 over n, we arrive at

$$\frac{V''}{V}(1-\phi_{lin}'') = \frac{(\tau-2)(1-\phi_{lin})}{n_1^{-(\tau-1)} - n_2^{-(\tau-1)}}\int_{n_1}^{n_2}\frac{n^{-(\tau-1)}}{1 + r\exp\{\sigma n\}}\,dn \quad (3.19)$$

We now have, along with eq 3.14, two nonlinear simultaneous equations with two unknown quantities ϕ_{lin}' and ϕ_{lin}''. The conditions for the coexistence of phases with different compositions may be determined by solving these equations for given values of ϕ_{lin}, n_1, and n_2 and varying χ.

3.3. The Cloud Point Curve. We shall now turn our attention to the cloud point curve (CPC), defined by the set of χ values for which phase separation first occurs for any given ϕ_{lin}; this should not be mistaken for the coexistence curve. On the CPC one of the phases, the "principal" phase, has the same characteristics as the bulk phase; i.e., for $\phi_{lin} > \phi_{lin}^{crit}$ (the subcritical branch of the CPC) the principal phase is linear-rich and the incipient phase is branch-rich, and for $\phi_{lin} < \phi_{lin}^{crit}$ (the supercritical branch of the CPC) the principal phase is branch-rich and the incipient phase is linear-rich. Under these conditions, eqs 3.14 and 3.15 can be rearranged to give[13,14]

$$\frac{\sigma}{2}(1+\nu_0) + \left(1 - \frac{1}{\bar{n}_n}\right) - \nu_0\left(1 - \frac{1}{\bar{n}_n''}\right) + \left(\frac{1}{1-\phi_{lin}} - \frac{1+\nu_0}{2}\right)\ln\left(\frac{\phi_{lin}}{\phi_{lin}''}\right) = 0 \quad (3.20)$$

in which the parameters of the incipient phase are denoted by double primes and those of the principal phase, being identical to those of the bulk phase, are denoted without primes. In eq 3.20

$$\nu_0 = (1-\phi_{lin}'')/(1-\phi_{lin}) \quad (3.21)$$

is the ratio between the volume fraction of the branched polymer in the incipient and principal phases. The former can be expressed in terms of the latter as

$$1 - \phi_{lin}'' = \int_{n_1}^{n_2}\phi(n)\exp\{-\sigma n\}\,dn \quad (3.22)$$

and the number-average degree of polymerization in the incipient phase is given by

$$\bar{n}'' = \int_{n_1}^{n_2}\phi(n)\exp\{-\sigma n\}\,dn \Big/ \int_{n_1}^{n_2} n^{-1}\phi(n)\exp\{-\sigma n\}\,dn \quad (3.23)$$

Equation 3.20 can be solved for a given α to find ϕ_{lin}'' and the corresponding value of χ can then be found from eq 3.18. By varying the value of σ, the CPC for fixed values of n_1 and n_2 may be determined.

On the supercritical branch of the CPC, for which $\sigma > 0$, eqs 3.22 and 3.23 can be conveniently, from a computational viewpoint, expressed in terms of the incomplete gamma function,

$$\int_0^x n^{-z}\exp\{-n\}\,dn \equiv \gamma(z,x) \quad (3.24)$$

as

$$1 - \phi_{lin}'' = \frac{(\tau-2)(1-\phi_{lin})}{n_1^{2-\tau} - n_2^{2-\tau}}I_0 \quad (3.25)$$

and

$$\frac{1}{\bar{n}_n''} = \frac{1}{\tau-1}\left\{\frac{n_1^{1-\tau}\exp\{-\sigma n_1\} - n_2^{1-\tau}\exp\{-\sigma n_2\}}{I_0} - \sigma\right\} \quad (3.26)$$

where

$$I_0 = \frac{1}{\tau-2}\{[n_1^{2-\tau}\exp\{-\sigma n_1\} - n_2^{2-\tau}\exp\{-\sigma n_2\}] - \sigma^{\tau-2}[\gamma(\tau-2,\sigma n_2) - \gamma(\tau-2,\alpha n_1)]\} \quad (3.27)$$

Equations 3.25–3.27 are well behaved in the limit of $n_2 \to \infty$; hence an "exact" numerical solution for the CPC may be found at the gel point for the supercritical branch.

However, for the subcritical branch of the CPC, i.e., $\sigma < 0$, eq 3.22 diverges for large n_2. One consequence of this is that any algorithm for finding the solution breaks down at finite n_2. Such behavior has been discussed extensively by Solc in the context of the logarithmic normal distribution function,[15] and the results can be quite generally applied to any "diverging" distribution function. The term diverging is used here to describe any distribution function which converges more slowly than any exponential $\exp\{-ax\}$; the power law distribution that we are considering is certainly an example of such behavior. It was predicted that in the limit of $n_2 \to \infty$, the CPC is superimposed onto the spinodal curve, i.e., is given by eq 3.7, and the composition of the two phases becomes identical.

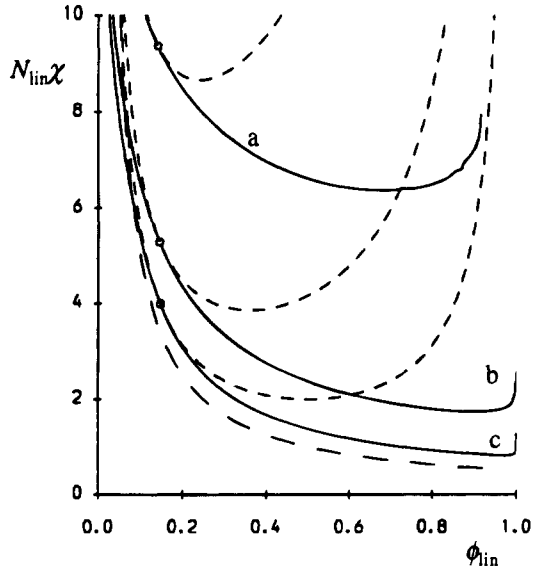

Figure 3. Cloud point curves (—), spinodal curves (- - -), and critical points for $n_1 = 0.01$ and (a) $n_2/n_1 = 10^2$, (b) $n_2/n_1 = 10^3$, and (c) $n_2/n_1 = 10^4$. The spinodal curve is plotted in the limit of the gel point (– – –).

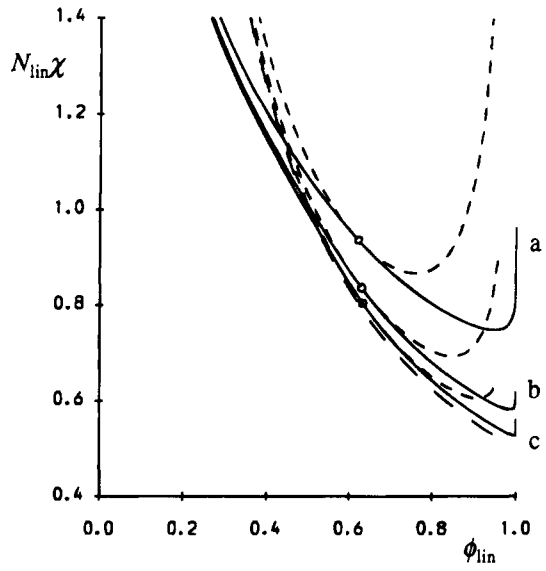

Figure 4. Same as Figure 3 but with $n_1 = 1.0$.

In this context it is interesting to note that for $\tau < 2.5$ there is no subcritical branch to the CPC for $n_2 \rightarrow \infty$, as the critical point tends to $\phi_{lin} = 1$ (see section 3.1). Hence the entire phase diagram can be computed numerically. Consequently, we can define a second type of diverging distribution function as one which converges slower than $n^{-1.5}\exp\{-an\}$ and has no meaningful subcritical branch to its CPC for $n_2 \rightarrow \infty$. One may expect such behavior in a polymer approaching the gel point in solution for which the classical statistics do not apply.

We are now at a stage where the evolution of the phase diagram during the curing process may be determined by calculating the cloud point curve and the spinodal curve for increasing values of n_2 at fixed n_1. A closer inspection of the actual structures that might be expected can then be found by solving the equations for the coexistence curves.

4. Results

We chose two values of n_1 (0.01 and 1.0); the former corresponds to the mixing of low molecular weight epoxy with high molecular weight polymer, and the latter to the molecular weights of both components being the same, prior to cross-linking of the epoxy. For both of these we calculated the CPC for three different n_2/n_1 ratios (10^2, 10^3, and 10^4); the results are shown in Figures 3 and 4 along with the spinodal curves and critical points. In all calculations we chose the classical exponent, $\tau = 2.5$. We have also plotted the spinodal curve in the limit of the gel point, illustrating the fact that it appears that the CPC tends toward this curve in the same limit, providing further support for the predictions of Solc. In Figures 5 and 6 we plot the "shadow curves" corresponding to Figures 3 and 4, defined by the locus of points representing the volume fraction of linear polymer in the incipient phase at the minimum value of χ at which phase separation occurs. Again it can be seen that the subcritical branch of these curves appears to be approaching the spinodal limit. The supercritical branch of the CPC for $n_2 \rightarrow \infty$ lies very close to that for $n_2/n_1 = 10^4$ and has not been included for the sake of clarity.

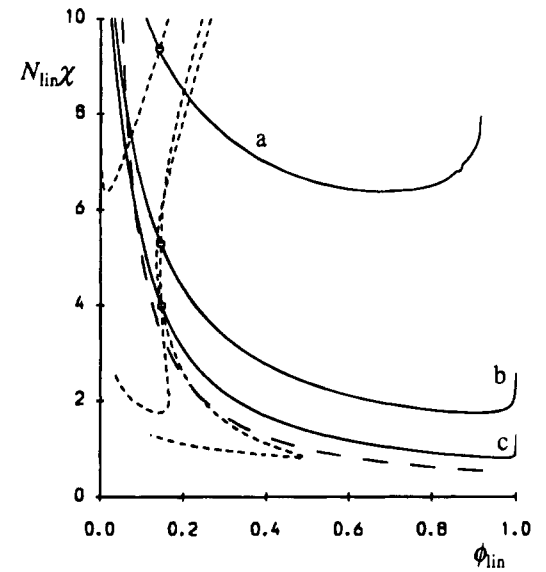

Figure 5. Shadow curves and CPC corresponding to Figure 3.

The coexistence curves for $n_1 = 0.01$ and each of the n_2/n_1 ratios for $\phi_{lin} = 0.25$, 0.5, and 0.75 are shown in Figures 7, 8, and 9. The composition of the linear-rich phases can be seen to alter very little as the value of χ is increased. The distribution of the branched polymer component, i, into the linear-rich and branch-rich phases for any ϕ_{lin}' and ϕ_{lin}'' may be found using eq 3.16 and

$$\frac{V'}{V}\phi_i' = \frac{\phi_i}{1 + r^{-1}\exp\{-\alpha n\}} \tag{4.1}$$

The resultant curves for $n_1 = 0.01$ and $n_2/n_1 = 10^2$, 10^3, and 10^4 at various values of χ for $\phi_{lin} = 0.5$ are shown in Figures 10, 11, and 12, respectively.

For values of χ close to the CPC the ratio diverges exponentially, as expected. Further away from the CPC the exponential divergence is cut off and the ratio becomes constant; this is particularly evident for $n_2/n_1 = 10^3$ and 10^4.

5. Discussion

There is clearly much similarity between the phase diagrams of Figures 3 and 4. In each case the region of

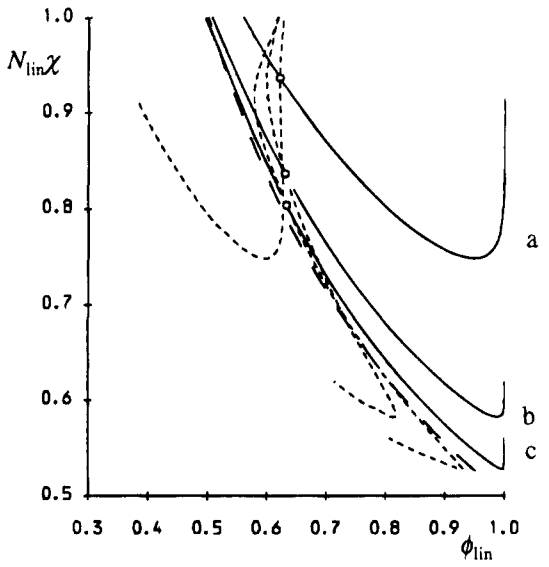

Figure 6. Shadow curves and CPC corresponding to Figure 4.

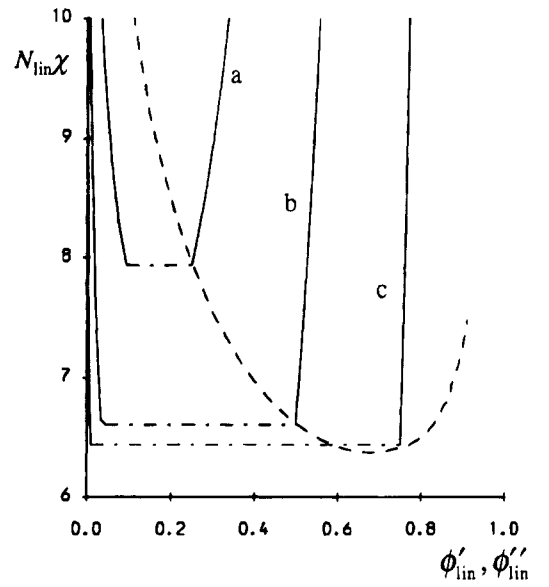

Figure 7. Coexistence curves (—) and the cloud point curve (- - -) for $n_1 = 0.01$ and $n_2/n_1 = 10^2$: (a) $\phi_{lin} = 0.25$; (b) $\phi_{lin} = 0.5$; (c) $\phi_{lin} = 0.75$. Sample tie lines (— • —) have been drawn.

incompatibility increases in size as curing proceeds, as would be expected. The shape of the cloud point curve alters dramatically. In particular, the area of the metastable region for $\phi_{lin} > \phi_{lin}^{crit}$ increases significantly as n_2 initially increases; however, the spinodal eventually "catches up" with the CPC, and the region of metastability becomes very small as the gel point is approached. The consequence of this is that any blend with such a composition that is initially miscible is likely to spend a long time in the metastable region during the curing process, and hence phase separation will occur by nucleation and growth, with the resultant morphology being that of an impact-resistant plastic. The metastable region above the supercritical branch of the CPC is always quite small.

In order to achieve a cocontinuous morphology, it is clearly necessary to identify the critical point of the blend and work very closely to this composition. The advantage of a branched polymer which obeys classical statistics is that its critical point does not vary much with n_2, and hence it is not necessary to know at what

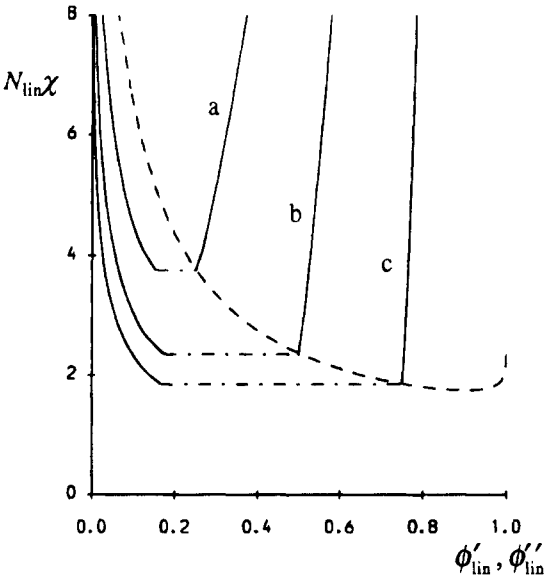

Figure 8. Same as Figure 7 but with $n_2/n_1 = 10^3$.

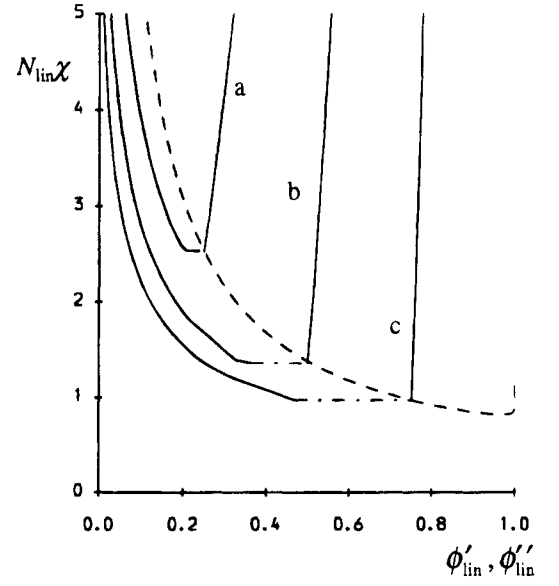

Figure 9. Same as Figure 7 but with $n_2/n_1 = 10^4$.

stage of curing the blend becomes immiscible in order to know the correct composition. However, this will present problems if there is even a slight deviation from classical behavior; hence it is desirable to work with thermosets comprised of long-chain polymers in order to achieve the greatest control over, and knowledge of, the behavior of the blend. Combining the curing process with a temperature quench (or jump for LCST behavior) may also ensure that the blend is brought into the spinodal region before any significant phase separation occurs.

An interesting feature of the coexistence curves is that the composition of the branch-rich phase always lies outside of the corresponding cloud point curve whereas that of the linear-rich phase always lies inside. This may at first seem a little surprising because of the apparent instability of the linear phase; however, it must be noted that the molecular weight distribution of the branched polymer is very different in each phase from the bulk distribution. Each phase must now be considered individually and will possess its own phase diagram. These "secondary" phase diagrams for each composition will be very different from those that we have calculated.

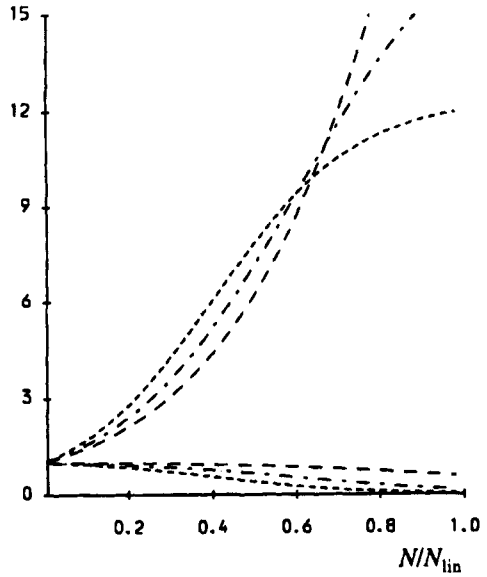

Figure 10. Distribution of the branched polymer into the branch-rich (upper set of curves) and linear-rich (lower set of curves) phases, plotted as $\phi''(N)/\phi(N)$ and $\phi'(N)/\phi(N)$, respectively, for $n_1 = 0.01$, $n_2/n_1 = 10^2$, $\phi_{lin} = 0.5$, and various values of χ: (– – –) $\chi N_{lin} = 7.00$; (– · – ·) $\chi N_{lin} = 8.00$; (- - -) $\chi N_{lin} = 9.00$.

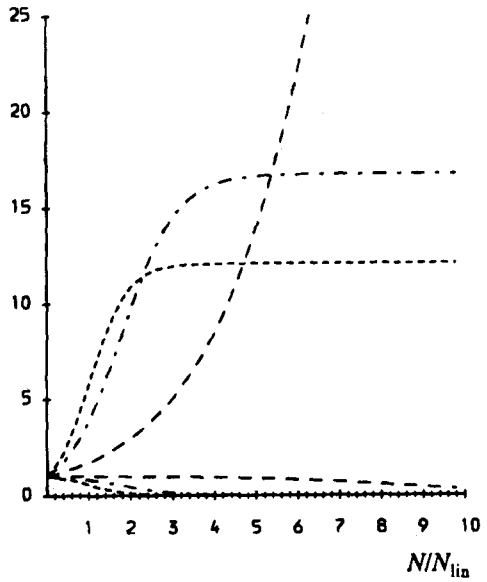

Figure 11. Same as Figure 10 but with $n_2/n_1 = 10^3$. The χ values are (– – –) $\chi N_{lin} = 2.50$, (– · – ·) $\chi N_{lin} = 4.00$, and (- - -) $\chi N_{lin} = 5.00$.

It is also surprising that the overall volume fraction of the linear-rich phase changes very little as χ varies over a large range above the CPC. This is indicated by the steepness of all coexistence curves. What has effectively happened is that the larger branched polymers have been segregated almost exclusively into the branch-rich phase, and hence the upper cutoff for the distribution function of the branched polymer has been reduced within the linear-rich phase.

The distribution of the branched polymer in each of the two phases, as illustrated in the examples of figures 10–12, shows unsurprising behavior: the larger branched polymers fractionate preferentially into the branch-rich phase, and the those within the linear-rich phase are mostly the smaller branched polymers. Note that in our approximation the latter would include the curing agent, which has a low molecular weight compared to any cross-linked branched polymer. So al-

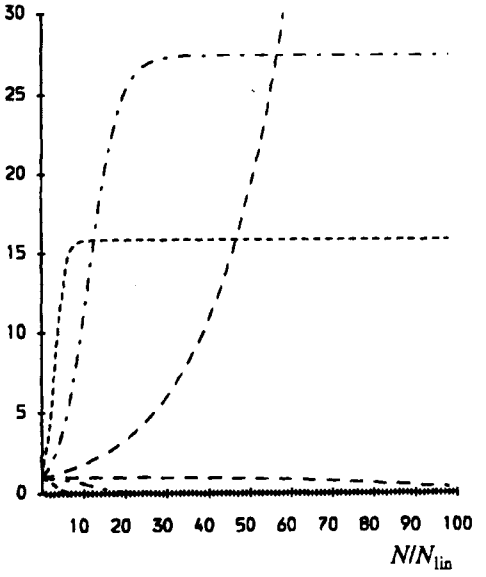

Figure 12. Same as Figure 10 but with $n_2/n_1 = 10^4$. The χ values are (– – –) $\chi N_{lin} = 1.40$, (– · – ·) $\chi N_{lin} = 2.00$, and (- - -) $\chi N_{lin} = 3.00$.

though the branch-rich phase is closer to the gel point, reactions within the linear-rich phase become more likely, and it is not necessarily the former phase which will gel first.

The possibility of a two-stage phase separation process occurring after a quench from the one-phase region into the two-phase region due to noninstataneous temperature changes, such that the blend may spend some time in the metastable region before crossing into the unstable region, has previously been discussed by Binder.[21] However, little evidence exists to support this idea, partly due to the difficulty of measuring the dynamics of nucleation and growth. For the systems we have been considering, such behavior is not only possible but probable and warrants further discussion.

There are two reasons that a two-stage separation process may occur; either the blend first passes into the metastable region and then into the unstable region such that some nucleation and growth precedes spinodal decomposition or, more interestingly, the composition of the coexisting phases changes due to continued cross-linking such that they themselves become unstable. The controlling factors behind the different processes are essentially the location of the composition with respect to the critical point and the proximity of the branched polymer to its gel point when the blend crosses into the two-phase region. We now look at some of these processes qualitatively.

Let us consider an un-cross-linked thermoset which is blended with a thermoplastic at a temperature within the one-phase region of the phase diagram and composition close to the critical composition (again we assume that classical statistics describe the distribution of the branched polymer such that the critical composition does not vary much during curing). After a certain degree of cross-linking has occurred so that the blend is no longer within the one-phase region, the initial phase separation process is spinodal decomposition from the growth of concentration fluctuations. The blend crosses into the unstable region after spending no, or a negligible amount of, time in the metastable region. As phase separation proceeds, the different compositions of branched polymer within each phase also continue to cross-link. While these compositions are initially

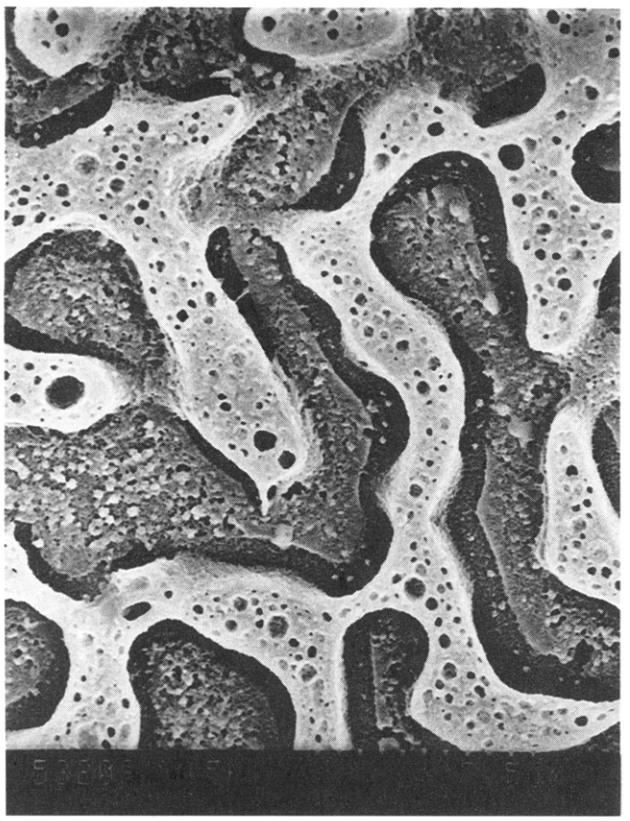

Figure 13. Electron micrograph of a thermoset/thermoplastic (epoxy/polysulfone (70/30)) polymer blend clearly showing a primary spinodal structure and secondary phase-separated nucleated sites within each of the cocontinuous phases.

stable, the increase of molecular weight of the branched polymer may induce a secondary phase separation within one or both phases. It is unlikely that the compositions of the coexisting phases are such that they are close to the critical points of their own secondary phase diagrams; hence any secondary phase separation will probably be via nucleation and growth. In Figure 13 we can see this behavior in a blend of epoxy and reactively terminated polysulfone in which secondary phase separation has occurred within both of the initial coexisting phases. The thermoplastic-rich (darker) phase has been etched away. Within the cocontinuous morphology can be seen spherical, secondary nucleated regions of thermoplastic in epoxy and epoxy in thermoplastic. This is the typical behavior of a blend which undergoes its first separation in the critical region of its phase diagram. From characterization of this blend it is known that the initial phase separation occurred well before the gel point. A similar phenomenon has been observed by Donatelli et al.[6] in a polystyrene/styrene−butadiene blend.

If, however, phase separation takes place when the branched polymer is close to the gel point, then both the initial and secondary phase separation will be via spinodal decomposition due to the negligible size of the metastable region.

Another possibility that can be seen from the coexistence curves is that the composition of the branch-rich phase is such that it may remain stable up to the gel point as it is very much to one side of the phase diagram; i.e., its volume fraction of branched polymer is much greater than the volume fraction of linear polymer. However, the linear-rich phase will almost certainly become unstable, as the reduced upper cutoff, noted earlier, increases once again as cross-linking resumes. Hence secondary phase separation may occur within just the linear-rich phase.

Finally, if the blend is not close to the critical composition and the branched polymer is not close to the gel point, then the initial phase separation will be nucleation and growth. This may become spinodal decomposition if the blend phases into the unstable region quickly enough. All manner of secondary phase separations are also possible; in fact, the possibilities are almost limitless.

In principle, a third, or even fourth, phase separation is possible; however, this is unlikely to occur prior to gelation and has never been observed. Of course, if one phase gels before the other, then the resultant morphology will be complicated by the effects of the elastic energy of the network on one phase while the other retains translational freedom. Such considerations are beyond the scope of this discussion.

6. Conclusions

We have shown that the behavior of the critical point is very unusual and strongly dependent on the exponent of the power law distribution function of the branched polymer. Hence a knowledge of the critical point prior to cross-linking and the exponent of the branched polymer distribution function during cross-linking will enable good qualitative predictions about the behavior of the blend during cross-linking.

The quantitative features of the spinodal curve at different stages of the cure process are unsurprising; however, the behavior of the example CPC's and coexistence curves does show some unusual features that would not, a priori, have been expected. It is clear that a full appreciation and understanding of the phase behavior of linear/branched polymer blends can only be gained by the theoretical analysis that we have presented in this paper; i.e., while the spinodal curves give a useful measure of various aspects of the phase diagram, they do not convey some of the important details which inevitably affect the resultant morphologies of such blends.

We have also shown that some secondary phase separation is not only possible but highly probable; it remains to be seen whether this has important consequences, beneficial or otherwise, for the mechanical and physical properties of thermoplastic/thermoset blends.

We look forward to experiments on well-characterized blends of cross-linked and linear polymers which simultaneously monitor the degree of reaction (e.g., by rheology) and phase separation (e.g., by light scattering). It will be particularly instructive to know how good our assumption of the power law distribution for branched polymers is for linear/branched blends.

Acknowledgment. We wish to thank R. Choudhery, S. Elliniadis, J. S. Higgins, T. McGrail, and S. Rostami for useful discussions and ICI for providing financial support for this project.

References and Notes

(1) Flory, P. J. *J. Chem. Phys.* **1942**, *10*, 51.
(2) Huggins, M. L. *Ann. N.Y. Acad. Sci.* **1942**, *42*, 1.
(3) Sanchez, I. *Annu. Rev. Mater. Sci.* **1983**, *13*, 387.
(4) Yamanaka, K.; Inoue, T. *Polymer* **1989**, *29*, 321.
(5) Acevedo, M.; de Abajo, J.; de la Campa, J. G. *Polymer* **1991**, *32*, 2210.
(6) Donatelli, A. A.; Sperling, L. H.; Thomas, D. A. *Macromolecules* **1976**, *9*, 671.
(7) Teng, K. C.; Chang, F. C. *Polymer* **1993**, *34*, 4291.

(8) Binder, K.; Frisch, H. L. *J. Chem. Phys.* **1984**, *81*, 2126.
(9) Donatelli, A. A.; Sperling, L. H.; Thomas, D. A. *J. Appl. Polym. Sci.* **1977**, *21*, 1189.
(10) Williams, R. J. J.; Borrajo, J.; Adabbo, H. E.; Rojas, A. J. *Abstracts of Papers*, 186th National Meeting of the American Chemical Society, Washington, DC, 1983; No. 96.
(11) Clarke, N.; McLeish, T. C. B. *J. Chem. Phys.* **1993**, *99*, 10034.
(12) Tanaka, F.; Stockmayer, W. H. *Macromolecules* **1994**, *27*, 3943.
(13) Koningsveld, R.; Staverman, A. J. *J. Polym. Sci., Part A2* **1968**, *6*, 325.
(14) Solc, K. *Macromolecules* **1970**, *3*, 665.
(15) Solc, K. *Macromolecules* **1973**, *6*, 819.
(16) Flory, P. J. *Principles of Polymer Chemistry*; Cornell University Press: Ithaca, NY, 1953.
(17) Stockmayer, W. H. *J. Chem. Phys.* **1944**, *12*, 45.
(18) Stauffer, D.; Coniglio, A.; Adam, M. *Adv. Polym. Sci.* **1982**, *44*, 103.
(19) De Gennes, P.-G. *J. Phys. (Paris)* **1977**, *38*, 355.
(20) Gibbs, J. W. Collected Works; Yale University Press: New Haven, CT, 1948; Vol. 1, p 65.
(21) Binder, K. *Materials Science and Technology: Phase Transformations in Materials*; Haasen P., Ed.; VCH: Weinheim, 1990; Vol. 5, Chapter 7.

MA946167S